

used for the measurements with stabilized image acquisition parameters. Epicardial vessels on the angiograms were masked out with an automatic multiscale vessel detection algorithm which analyses eigenvalues of the Hessian matrices of image points. Time-density curves (TDC) were recorded in infarct-related polygonal regions, selected by a cardiologist experienced in the analysis of coronary angiograms. Frequencies higher than 0.6 Hz were removed from the TDC to eliminate artifacts from cyclic heart contractions. G_{\max} was defined as maximal amplitude of the TDC, T_{\max} is the time to reach G_{\max} . Both values were automatically computed from the resulting curve (Fig. 1). Perfusion was characterized with G_{\max}/T_{\max} . This novel videodensitometric method has been compared with enzymatic infarct size as expressed by sum of CK release, 90-min ST-segment resolution and ejection fraction 3 days after successful revascularization.

Results

All patients underwent successful recanalization of the occluded epicardial artery within 8 h from the onset of symptoms. Bland & Altman analysis reveals a reliable interobserver agreement in our computerized method. Significant linear correlations were found between G_{\max}/T_{\max} and enzymatic infarct size ($R = -0.445$, $P < 0.001$), ST-segment resolution ($R = 0.364$, $P = 0.004$) and ejection fraction ($R = 0.278$, $P = 0.029$). Optimal cut-off values have been determined for TIMI Myocardial Perfusion Grade (TMP), G_{\max}/T_{\max} to predict sum of CK $< 5,000$ U/l (Fig. 2). The computerized method increased sensitivity (73–85%) and specificity (76–79%) as well. G_{\max}/T_{\max} without vessel masking did not improve results of ROC analysis significantly, compared to TMP.

Conclusion

Myocardium selective videodensitometric perfusion measurement, characterized by G_{\max}/T_{\max} of the time-density curve in the infarct related myocardial area is a reliable parameter to assess recovery of myocardial function during the time of acute coronary intervention. Vessel masking improves the results compared to simple densitometric analysis. Therefore, this novel method could be used to immediately assess myocardial viability after recanalisation, or as an objective end-point in clinical trials of new interventional devices and drugs, in place of the visual classification grades.

Automated coronary artery segmentation using morphological operators

Lin C.-C.¹, Kuo W.-J.¹

¹Yuan Ze University, Department of Information Management, Chung-Li, Taiwan

Keywords Coronary angiogram · Morphological · Segmentation
Purpose

Coronary angiogram is one of the most valid methods for diagnosing the presence of coronary artery disease. Therefore, the development of digital image analysis techniques for the objective and precise analysis of coronary angiograms become an important research. The problem of coronary image analysis is to find accurate information for the dimensions of the arteries to construct a structural description of the coronary tree to make the reliable extraction of higher level diagnostic information possible. However, vessels may be broken into several disconnected components and discontinuities may occur at bifurcation or stenosis points. To achieve the purpose of providing accurate information, it is imperative to develop excellent segmentation and automated techniques for angiogram image analysis. The purpose of this study is to propose an algorithm to extract the skeletons and borders of coronary arteries in digitalized angiograms automatically.

Methods

In this paper, we proposed an automatic tubular enhancement algorithm based on eigenvalue analysis of the Hessian matrix to extract the skeletons and borders of coronary arteries in digitalized

angiograms. Morphological majority filter is also applied in the segmented image to smooth the contours and to remove some small isolated regions. Initially, the approximate contour of coronary angiogram is roughly estimated by region growing and edge dilation. The purpose of this step is to depict the main contour of the coronary simply without considering its complexity of background. The rudimentary coronary is then segmented into closed fractions by edge skeleton growing iteratively. No matter how other closed fractions will affect and under-segmentation caused by the complicated background, this step ensures that most of the fractions inside the coronary will be closed. The temporary fraction map is further enhanced by the eigenvalue analysis of the Hessian matrix to highlight tubular structures from tissues and background noises in angiogram images. Then, the retained fractions are filtered by the Otsu dynamic threshold method iteratively. In this stage, the true fractions of the coronary will grow along the coronary to form the main object of the coronary. Finally, the segmentation result will be achieved by performing the intersection between the main object and the dilated edges.

Results

To demonstrate the correctness of the proposed method in detecting the artery skeletons and segmentation result, the proposed method was examined using a set of clinical coronary angiogram images. Both of the right and left coronary angiograms were included in the data sets. Simulation results showed that we were able to extract the principle coronary artery contours and centerlines by the proposed method successfully. Moreover, the segmentation results preserve the original coronary artery width while with less background noises. It is clear that the borders are successfully and automatically extracted. Especially, the proposed method performed well in low-contrast noisy angiograms with many artery crossings.

Conclusions

In recent clinical researches, it has been revealed that coronary artery analysis becomes important indicators of coronary heart disease. In this study, an automatic tubular enhancement algorithm based on eigenvalue analysis of the Hessian matrix was proposed to extract the skeletons and borders of coronary arteries in digitalized angiograms. Experiment result showed that the proposed method can successfully extract the principle coronary artery contours and centerlines. The segmented results can be further used to analyze the diagnostic information of coronary artery. Through the analysis of coronary artery, we hope that the cardiopathy could be diagnosed earlier to get the prevention or treatment better. Further research is aimed in the direction of quantitative analysis of coronary arteries for the development of computer-aided diagnosis (CAD) system.

Acknowledgments

This work was supported by the National Science Council, Taiwan, Republic of China, under Grant NSC-96-2221-E-155-063-MY3

A comparison study of two reconstruction methods for gated cone-beam CT

Hartl A.¹, Yaniv Z.²

¹Technical University of Munich, Computer Aided Medical Procedures, Garching, Germany

²Georgetown University Medical Center, Imaging Science and Information Systems (ISIS) Center, Department of Radiology, Washington, DC, USA

Keywords Image-guided therapy · Surgical guidance · Cone-beam CT

Purpose

C-arm based Cone-Beam CT (CBCT) imaging enables the in situ acquisition of three dimensional images. In the context of image-guided interventions this technology has the potential to reduce the complexity of a procedure's workflow, with imaging and intervention carried out in the same location. For interventions carried out in the thoracic-abdominal regions, image acquisition while the patient is

freely respiring results in blurred images. To improve image quality, data is acquired either at breath-hold or using retrospective gating approaches, resulting in a 4D(space + time) reconstruction. To acquire a 4D CBCT image using retrospective gating, the acquired projection X-ray images are grouped into separate data sets based on their phase in the respiratory cycle. Standard reconstruction is then performed for each data set. Motion artifacts are reduced as the number of data sets is increased. On the other hand this also reduces the number of images in each data set which increases the reconstruction artifacts. Thus, it is not uncommon that multiple data acquisitions are performed so that each data set, corresponding to a respiratory phase, has a sufficient number of images for reconstruction.

In this work, we evaluate the quality of 4D CBCT reconstructions computed using the filtered back-projection method of Feldkamp–Davis–Kress (FDK), and simultaneous algebraic reconstruction (SART), using a simulation framework that mimics the current clinical CBCT acquisition protocol for soft tissue imaging.

Methods

To evaluate the effect of a reconstruction algorithm on the quality of 4D CBCT data we performed the following simulation study. We use a digital phantom composed of two spheres. The abdomen is represented by a stationary sphere and a target tumor is represented by a sphere performing sinusoidal modulated

Cranial–caudal motion with an amplitude of 20 mm. Amplitude magnitude is based on published studies describing respiratory motion of the liver. Simulated breathing frequencies were set to 15 and 18 breaths per minute, normal respiratory rates. We then generate Digitally Reconstructed Radiographs (DRR) using the projection parameters for soft tissue imaging from a clinical system, the Siemens Axiom Artis dFA. The resulting data set consists of 543 DRRs spanning 220°, with an acquisition time of 20 s.

For each of the breathing frequencies we evaluated the quality of the reconstruction algorithms using five and ten subsets per respiratory cycle, with projections binned according to their respiratory phase. Figure 1 shows the simulation setup with five bins and a respiratory rate of 15 breaths per minute.

Reconstructed images from each subset were compared to the known scene at that respiratory phase using normalized cross correlation (NCC), Pearson's r . That is, two images are equivalent if they follow a linear relationship. This reflects the equivalence between images mapped using the common radiologic window and level linear mapping. Finally, we also compared image quality of the SART method with an initial reconstruction obtained using the FDK method.

Results

In all reconstructions the SART algorithm exhibited a slightly higher correlation than the FDK method. When using five bins and a respiratory rate of 15 breaths per minute the FDK method had a NCC value of 0.71 and the SART had a value of 0.76. This setup was the most favorable, in that the subset sizes were the largest in our simulation study. When we increased the number of bins to ten the FDK

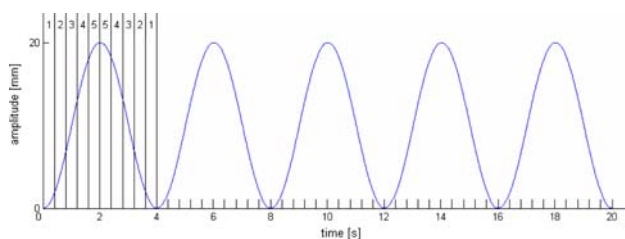


Fig. 1 Simulation setup with five bins and a respiratory rate of 15 breaths per minute. From left to right and top to bottom: ground truth; FDK; SART; and FDK followed by SART

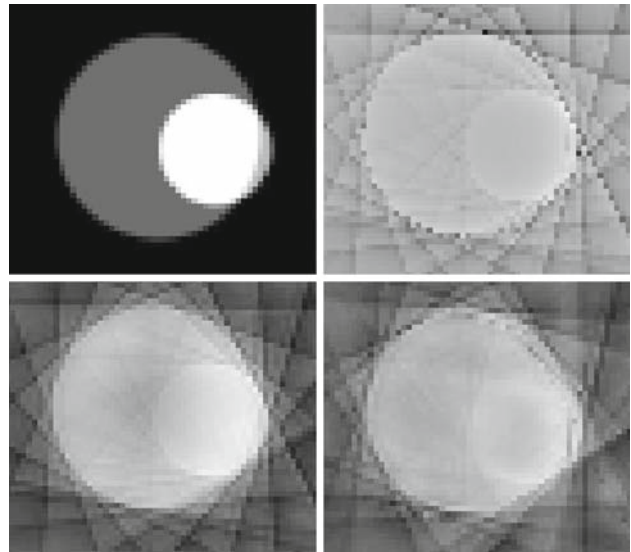


Fig. 2 Reconstruction results using 5 bins and 15 breaths per minute

method had an NCC value of 0.68 and the SART a value of 0.78, reflecting the sensitivity of FDK to the number of projection images. When we used five bins and a respiratory rate of 18 breaths per minute the FDK method had a NCC value of 0.73 and the SART a value of 0.75. When we increased the number of bins to ten the FDK method had a NCC value of 0.7 and SART had a value of 0.78. For the SART algorithm initialized with the FDK result we obtained similar values to SART, only with a reduced computational time. Figure 2 shows the results we obtained for reconstructions using 5 bins and 15 breaths per minute, from left to right and top to bottom: ground truth; FDK; SART; and FDK followed by SART.

For the FDK algorithm reconstructions took on average 1 min using 100 images. For the same data sets the SART algorithm took approximately 30 min. Finally, the combination of FDK followed by SART took approximately 15 min. It should be noted that we implemented the SART and FDK algorithms in a straightforward manner and did not optimize our code; as a result the running times of our reconstructions are not optimal.

Conclusion

Based on our simulations, we see that with the current clinical imaging protocol the SART method is able to produce better reconstructions. This is primarily due to the small number of unique images included in each subset. The fast acquisition time of 20 s with normal respiratory rates results in subsets that are acquired from a limited number of angles. While the number of images included in each subset is substantial they are concentrated around a limited number of viewing angles.

Based on these observations we will further investigate the use of the SART method to perform our reconstructions. We will focus on improving the implementation efficiency. This is a promising avenue as published works have shown that using hardware acceleration, with the graphics processing unit, SART reconstructions can be performed in near real time.

Algebraic reconstruction methods for GPU cone beam tomography

Frosio I.¹, Pedersini F.¹, Pasini A.², Bianconi D.², Borghese N.A.¹

¹University of Milan, Computer Science Department, Milan, Italy

²Cefla, Imola, Italy

Keywords Tomography · Algebraic methods · Graphic processor unit